DEFENSE TECHNICAL INFORMATION CENTER

Information for the Defense Community

DTIC® has determined on 2/24/12 that this Technical Document has the Distribution Statement checked below. The current distribution for this document can be found in the DTIC® Technical Report Database.

☒ **DISTRIBUTION STATEMENT A.** Approved for public release; distribution is unlimited.

☐ **© COPYRIGHTED.** U.S. Government or Federal Rights License. All other rights and uses except those permitted by copyright law are reserved by the copyright owner.

☐ **DISTRIBUTION STATEMENT B.** Distribution authorized to U.S. Government agencies only (fill in reason) (date of determination). Other requests for this document shall be referred to (insert controlling DoD office).

☐ **DISTRIBUTION STATEMENT C.** Distribution authorized to U.S. Government Agencies and their contractors (fill in reason) (date determination). Other requests for this document shall be referred to (insert controlling DoD office).

☐ **DISTRIBUTION STATEMENT D.** Distribution authorized to the Department of Defense and U.S. DoD contractors only (fill in reason) (date of determination). Other requests shall be referred to (insert controlling DoD office).

☐ **DISTRIBUTION STATEMENT E.** Distribution authorized to DoD Components only (fill in reason) (date of determination). Other requests shall be referred to (insert controlling DoD office).

☐ **DISTRIBUTION STATEMENT F.** Further dissemination only as directed by (insert controlling DoD office) (date of determination) or higher DoD authority.

Distribution Statement F is also used when a document does not contain a distribution statement and no distribution statement can be determined.

☐ **DISTRIBUTION STATEMENT X.** Distribution authorized to U.S. Government Agencies and private individuals or enterprises eligible to obtain export-controlled technical data in accordance with DoDD 5230.25; (date of determination). DoD Controlling Office is (insert controlling DoD office).

Final Progress Report

Molecular Electronics for Flash Memory Production

Department of Defense Congressional Award

Sponsor Award Number: W911NF-10-1-0510

Principal Investigators:

J. Fraser Stoddart
Northwestern University
Department of Chemistry
2145 Sheridan Road
Evanston, IL 60208-3113

Email: stoddart@northwestern.edu
Phone: 847-491-3793
Fax: 847-491-1009

Chad A. Mirkin
Northwestern University
Department of Chemistry
2145 Sheridan Road
Evanston, IL 60208

Email: chadnano@northwestern.edu
Phone: 847-491-2907
Fax: 847-467-5123

Period Covered by this Report: August 24, 2010 to August, 24, 2011

Date of Report: December 28, 2011

Objectives

The specific objectives of this grant are — *(i) To develop bistable molecular switches on the scale of a few cubic nanometers, and (ii) To devise a means by which these nanoswitches can be fabricated in a precise and/or periodic manner with complete precision.*

Summary

The continued reduction of the feature density of memory chips has increased interest in the utilization of molecules as the functional elements in electronic memory devices because of the advantages they offer in terms of size compared to conventional circuit elements. The development of molecular electronic devices for memory applications in computing, however, continues to be an important challenge to researchers in nanoscience and nanotechnology, both from a fundamental and an applied standpoint. Molecular switch tunnel junctions (MSTJs), in which molecules are sandwiched between two electrodes, have been explored in the context of developing viable molecular electronic devices, but their behavior in these nanoscale junctions are complex and difficult to understand. One of the chief obstacles to understanding these physical phenomena arises from the inability to use conventional spectroscopic tools at the small length scales and low molecule concentrations (100's - 10,000's) within the junctions. To this end, we are employing On-Wire Lithography (OWL) as a platform for the development and rapid synthesis of devices for examining the *I-V* response of a variety of molecular electronic systems. As was outlined in our proposed deliverables timelines, we are focusing our efforts on three areas: (1) optimizing OWL to accommodate a variety of molecular wire systems, (2) correlating the *I-V* response with Raman spectroscopic signatures, and (3) incorporating these devices into large scale arrays. Specifically, we proposed the synthesis of a variety of molecular wires incorporating functional macrocycles, beginning the investigation of host-guest model systems, and optimizing the electrode for Raman activity and beginning to build structures demonstrating large Raman enhancement.

With the intent of investigating molecular switching systems in OWLs, we have designed and synthesized series of thiol-functionalized rigid linkers incorporating molecular recognition components — (1) an electron-rich crown ether composed of a hydroquinone derivative, (2) an electron rich crown ether, 1,4-benzo-1,5-naptho[36]crown-10 (BN36C10), which has higher affinity towards electron-deficient quest molecules such as methyl viologen ($BIPY^{2+}$), than the hydroquinone derivative and (3) an electron-deficient tetracationic cyclophane derivative which can bind to the electron-rich guest molecules such as 1,5 dioxynapthalene (DNP) and tetrathiafulvalene (TTF). In addition, we have also synthesized a rigid bis-terpyridine and thiol-functionalized terpyridine derivatives to investigate the metal-directed self-assembly of molecular wires within OWL-generated nanogaps. Recently, we have also completed synthesis of a redox controllable bistable molecular switch which exhibits photoinduced memory effect.

Concerning the incorporation of these functional molecules into OWL-generated nanogaps, we have successfully demonstrated bridging of the two gold electrodes by an α,ω-bisthiol-oligo(phenylene ethynylene) (**L2**) containing a BN36C10 functional group. The *I-V* response of the device is in analogous to previously investigated molecular systems without the BN36C10 moiety.

Accomplishments

Objective 1: Synthesis of Molecular Wires Incorporating Molecular Recognition Components

In order to understand fundamental principles in designing molecular memory devices based on (1) [2]pesudorotaxanes, (2) bistable donor-acceptor [2]catenanes and (3) bistable [2]rotaxanes, we have designed and are in the process of synthesizing series of rigid linkers incorporating these switchable subunits. We have successfully demonstrated the host-guest interactions within the nanogaps and correlated to spectroscopic signatures using Raman spectroscopy. This experiment allowed us to obtain direct spectroscopic evidence for the formation host-guest complexes. We will are currently implementing this principle to characterize more complex switches within the gaps.

To fully understand switching behavior of the bistable catenanes and rotaxanes, we first turned our attention to investigate the inclusion complexes of molecular wires incorporating both electron-deficient and electron-rich host components. This particular experiment allowed us to obtain spectroscopic information (Raman spectroscopy) from the segments of bistable catenanes and rotaxanes, therefore, allowing us to indentify the Raman signals of individual stations. We have designed and synthesized a series of linkers (**Figure 1**) functionalized with both electron-rich, **L1** and **L2**, and electron-deficient, **L3**$^{4+}$, components. Linkers **L1** and **L2** can bind selectively to the electron-deficient guest molecules and we have shown that when these molecular wires are assembled within the gaps, they show organic semiconductor type behavior, however, addition of DAP^{2+} alters their conducting properties.

The linkers **L1** and **L2** were synthesized as shown in Scheme 1. Thioacetyl functionalized extended phenylacetylene linker, **1**, can be obtained over five steps in relatively high yields using series of Sonagashira coupling reactions. First, 4-iodobenzenesulfonyl chloride was converted to 4-thioacetyliodobenzene and then iodine was replaced by acetylene group in the presence of

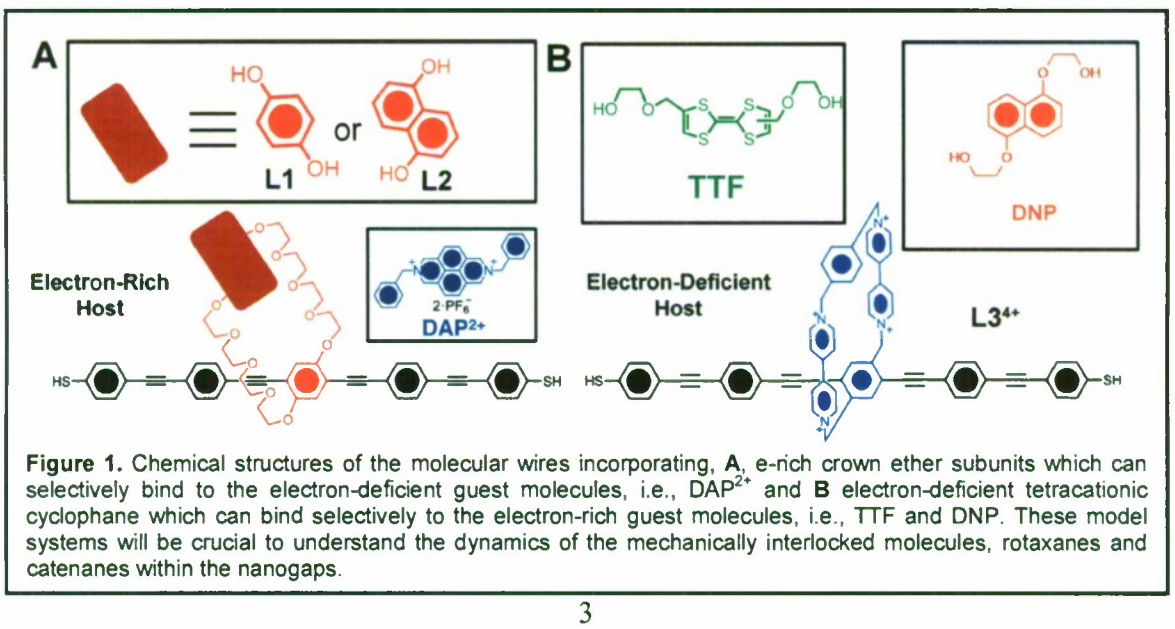

Figure 1. Chemical structures of the molecular wires incorporating, **A**, e-rich crown ether subunits which can selectively bind to the electron-deficient guest molecules, i.e., DAP^{2+} and **B** electron-deficient tetracationic cyclophane which can bind selectively to the electron-rich guest molecules, i.e., TTF and DNP. These model systems will be crucial to understand the dynamics of the mechanically interlocked molecules, rotaxanes and catenanes within the nanogaps.

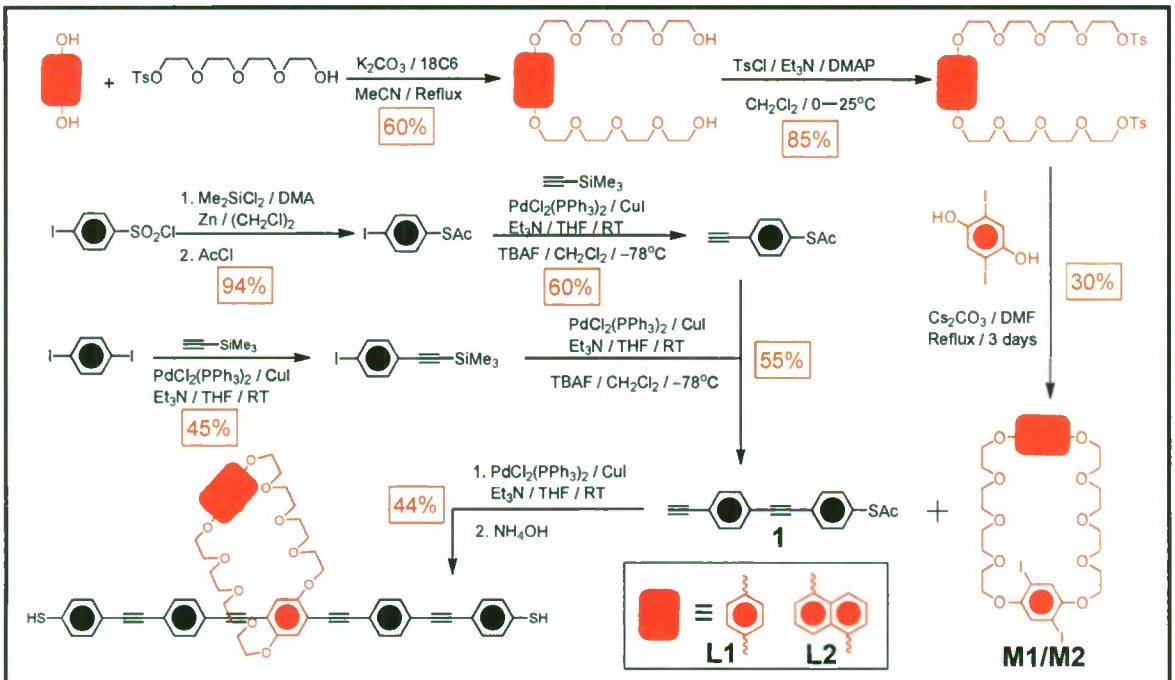

Scheme 1. Syntheses of molecular wires **L1** and **L2** incorporating electron-rich crown ether subunits.

trimethylsilylacetylene under Sonogashira coupling conditions followed by the deprotection of trimethylsilyl (TMS) group. This intermediate was then reacted with iodobenzene derivative, which was obtained upon mono-functionalization of 1,4-diiodobenzene with trimethylsilylacetylene, in the presence of Sonogashira coupling reagents and consequently followed by TMS deprotection to obtain the desired thioacetly-functionalized extended alkyne, **1**. The two macrocyclic precursors **M1** and **M2** were obtained by following the well-established

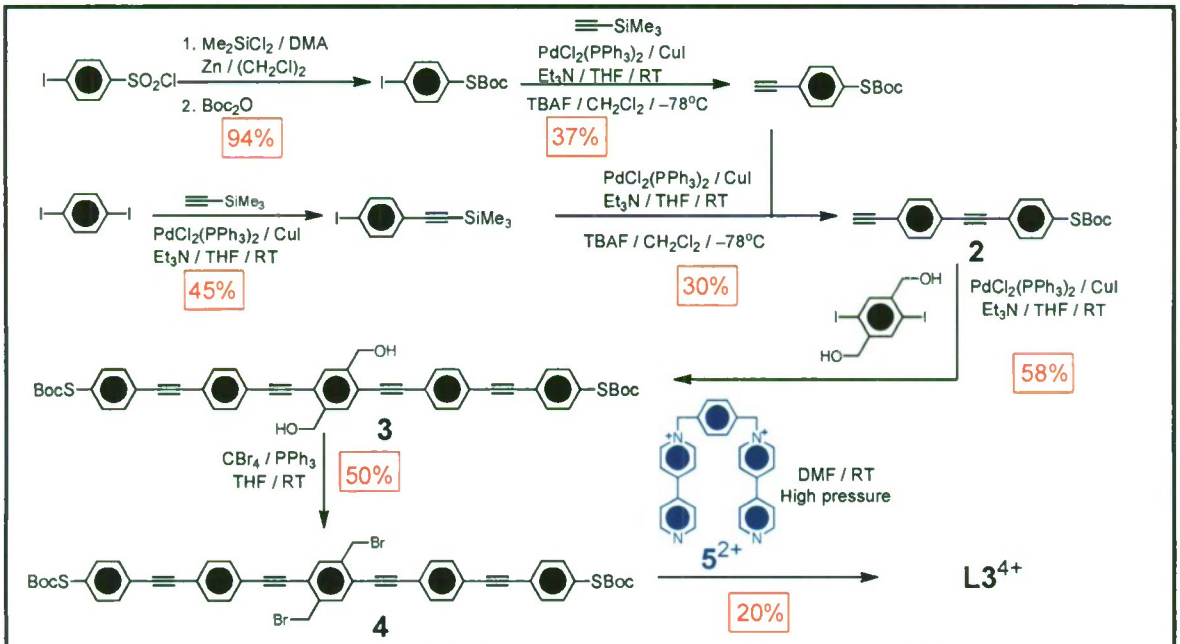

Scheme 2. Synthesis of molecular wire **L3**.4PF_6 incorporating electron-deficient tetracationic cyclophane.

macrocyclization procedures. Either 1,4-dioxybenzene (**M1**) or 1,5-dioxynapthalene (**M2**) was reacted with monotosylated tetraethyleneglycol, followed by the tosylation of hydroxyl groups prior to the macrocyclization reaction. Both macrocycles were obtained under high dilution conditions in the presence of 2,5-diiodohydroquinone. Finally, these macrocyles were reacted with the compound **1** under the Sonogashira coupling reaction conditions to yield thioacetyl-functionalized molecular wires **L1** and **L2**. The removal of acetyl groups to obtain free thiol groups was achieved using NH_4OH prior to the device fabrication in order to avoid the formation of disulfide bond.

Linker $\mathbf{L3}^{4+}$ is known to bind selectively to the electron-rich guest molecules, i.e., TTF and DNP. We have recently completed the synthesis of this linker and its solution-state characterization is in progress. The molecular wire $\mathbf{L3}^{4+}$ has been synthesized (**Scheme 2**) by following Sonagashira coupling conditions, followed by template-directed synthesis to form the tetracationic cyclophane. The compound **2** can be obtained over five steps in relatively good yields. The coupling of the compound **2** with 1,4-diiodo-2,5-hydroxymethylbenzene yielded the extended linker **3** in 58% yield. Then, the hydroxyl groups on the central aromatic unit were converted to bromide using CBr_4 and PPh_3 in THF to form the compound **4** in 50% yield. This bromomethyl-functionalized linker was then reacted with the compound $\mathbf{5}^{2+}$ in a high pressure reactor in order to form the linker $\mathbf{L3}^{4+}$ in 20% yield. It is important to note that *Boc* group was opted instead of acetyl in this case on account of the basic deprotections conditions required for the acetyl group. We will test its binding with electron-rich guest molecules within the gap.

Objective 2: Optimize OWL-Generated to Accommodate a Variety of Molecular Wires.

Improving the topographical roughness of nanowire electrode ends: During the course of our monthly research meetings, we eluded to further optimization of our nanowire smoothing protocol using qualitative insight derived from electron microscopy. For a more quantitative assessment, full characterization of freestanding nanowire arrays was done with atomic force microscopy (AFM). Verifying our previous conclusion, we determined that the updated technique resulted in a 25% improvement in RMS roughness down to 3 nm from 4 nm as was previously reported[1] (**Figure 2**). Owing to a decrease in the likelihood of electrical contact across these smoother gaps, we hypothesize an important increase in the final yield of working devices as a direct result of this significant improvement.

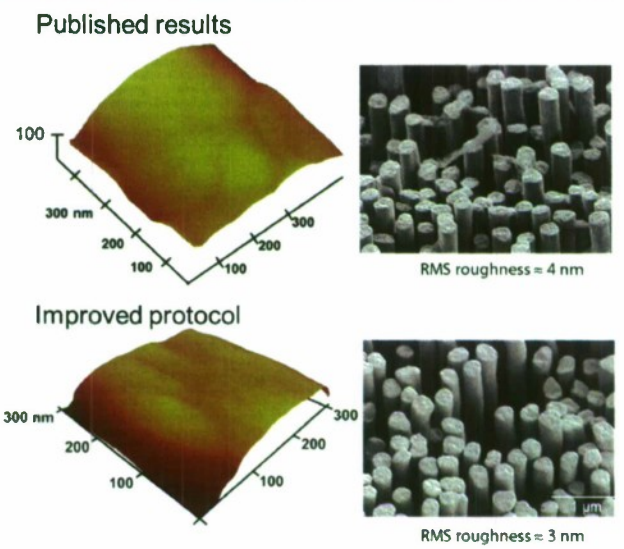

Figure 2. Representative AFM and corresponding SEM images of nanowire arrays with smooth ends. (Top) Using the previously published protocol for nanowire smoothing the RMS roughness values were ~4 nm. (Bottom) New instrumentation for the electrochemical deposition affords an automated process with fine control of charge passed during the requisite pulsing and subsequent oxidation of the nanowire surface. RMS roughness values are now ~3 nm. Scale bar is 1 μm.

Electrical investigation of host-guest complex formation within OWL-generated nanogap devices: As a demonstration of the ability to study molecular wires containing functional moieties (including those required for switching behavior), we have designed a model system to begin our investigation. From this point, we are currently investigating the effect of the addition of a known guest molecule (DAP^{2+}) in forming a host-guest complex. While this complex has been demonstrated and characterized in solution, the full investigation of its effect on charge transport in a working device remains an area of significant research effort. Our preliminary data illustrates the successful bridging of the nanoscale gap within the nanowire (**Figure 3**). From the *I-V* curve for this sample, we can observe dramatically different current response after the addition of the molecular wire. Based on previous investigation, we hypothesized that following the formation of the host-guest complex within the nanogap will result in rapidly diminished charge transport through the molecule as a result of the electron-deficient DAP^{2+} acting as an electron sink and absorbing electrons travelling through the molecular wire (**Figure 3B**). At the time of this report, we have successfully incorporated the guest molecule into the macrocycle that was contained within the OWL-generated nanogap. The electrical data is in agreement with our earlier hypothesis for all of the devices tested. We believe that this demonstration is an important stepping stone to being able to detect changes within the bistable rotaxane within the OWL-based molecular transport junctions.

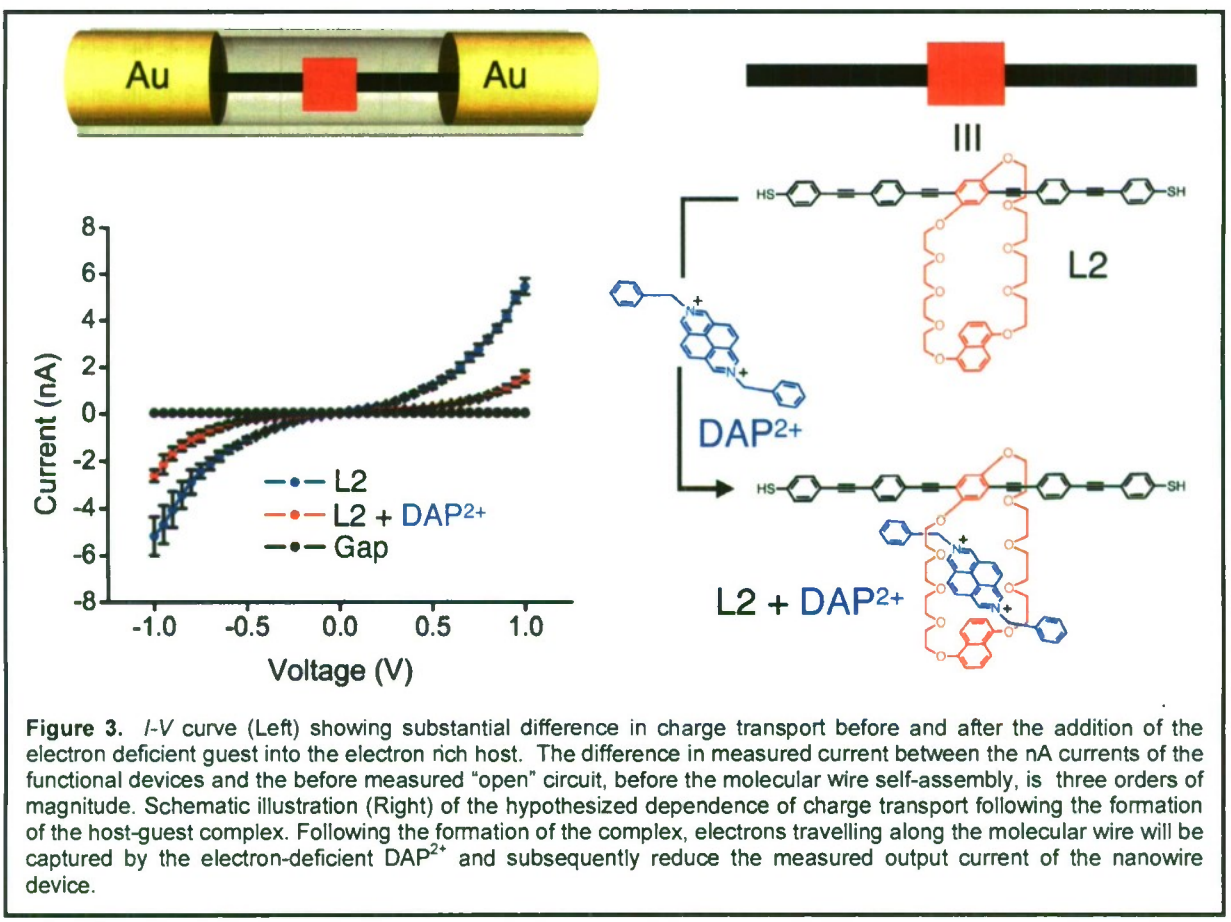

Figure 3. *I-V* curve (Left) showing substantial difference in charge transport before and after the addition of the electron deficient guest into the electron rich host. The difference in measured current between the nA currents of the functional devices and the before measured "open" circuit, before the molecular wire self-assembly, is three orders of magnitude. Schematic illustration (Right) of the hypothesized dependence of charge transport following the formation of the host-guest complex. Following the formation of the complex, electrons travelling along the molecular wire will be captured by the electron-deficient DAP^{2+} and subsequently reduce the measured output current of the nanowire device.

Objective 3: Correlate the *I-V* response with Raman spectroscopic signatures

Research efforts to achieve the correlated Raman spectroscopy to the electrical measurements proved to be a significant research challenge. Optimizing the nanowire geometry to produce large electric fields for the necessary SERS measurements was exceedingly difficult. The presence of metallic leads connecting these wires to microelectrodes further adds to the complexity of this system. Raman intensity data on the nanowire geometry dependence of 3 nm gap nanowires shows a very small signal to noise ratio (**Figure 4**). Ultimately, a different approach was required in order to fully demonstrate the successful functionalization of the OWL-based MTJs with the aforementioned functional OPE derivative to mitigate problems with meeting the signal to noise requirements.

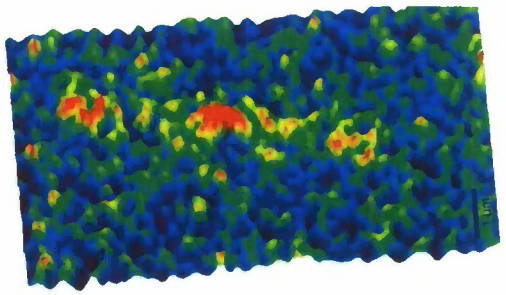

Figure 4. Raman intensity map illustrating the presence of a Raman hot-spot located in the center of the scan window with additional enhancement observed at the ends of the nanowire. While this is a reasonable starting point for the use of Raman coupled to electrical measurements, further optimization is required to enhance the signal to noise ratio.

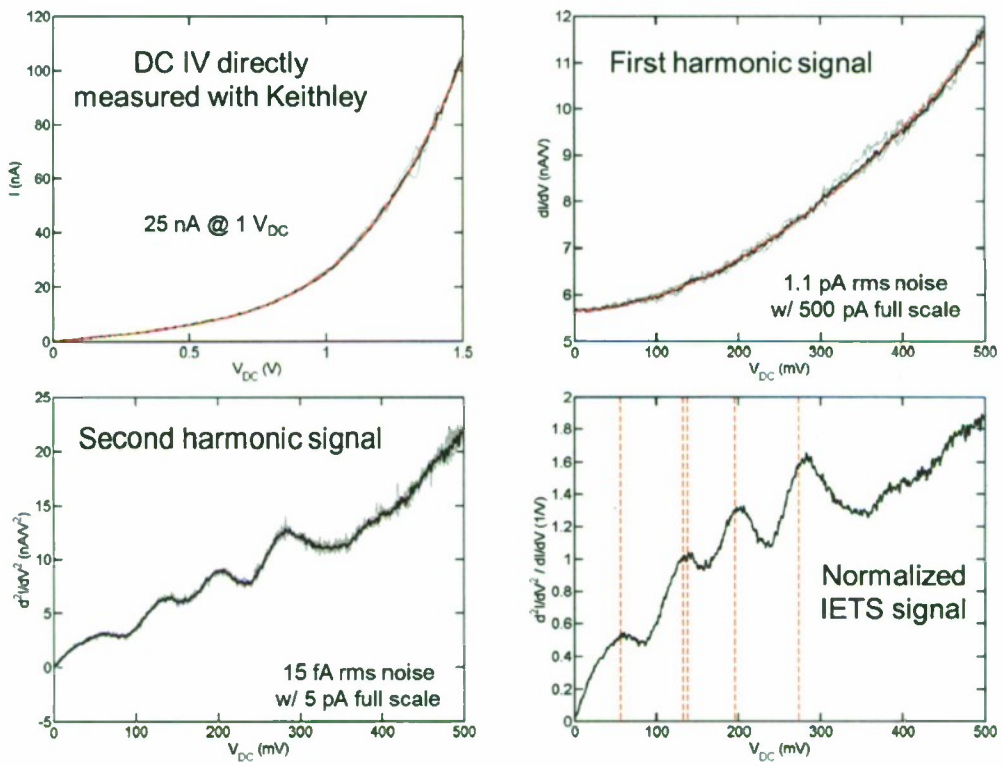

Figure 5: Analysis of the DC *I-V* curve is done sequentially measuring directly, the first harmonic ($\delta I/\delta V$), the second harmonic ($\delta I^2/\delta V^2$), and a normalization to remove the scale of the measured current. The red dashed lines represent notable vibrational modes from the Raman and Infrared spectra.

Inelastic electron tunneling spectroscopy (IETS) has been established as a viable technique to observe vibrational modes of conducting molecules sandwiched between metal electrodes. Further, utilizing this technique has been used within OPE system and allows for the observation of both infrared and Raman vibrational modes. Following the successful setup and installation of components required for testing, we began looking at how the OPE derivative behaves within the OWL-generated gap. We can confirm the presence of OPE by comparing to previously published results[2] (Figure 5). In the last panel of Figure 5 we show our IETS data with notable peaks collected by Raman and IR spectroscopy superimposed as red dashed lines. The agreement between the two spectroscopies is conclusive that we have successfully put our OPE derivative into the gap and work is ongoing to demonstrate that the incorporation of the guest molecule produce notable changes in the IETS data.

Objective 4: Synthesis of Building Blocks and Molecular Wires for the Investigation of Metal-Directed Self-Assembly within the OWL-Generated Nanogaps

In this project, we utilize the concept of metal-directed self-assembly based on the formation of metal complexes of terpyridine linkers. We hypothesize that this approach will not only provide us a modular system in which the structure of the linker can be changed easily without going through several synthetic steps, but also improve the yield of working devices. In addition, formation of these wires are expected to be independent of a gap size allowing us additional level of control in our devices, While this chemistry has demonstrated the formation of highly-conducting molecular wires on flat gold surfaces, in our design we are proposing to use this concept to bridge the OWL-generated nanogaps of varying sizes. The bisterpyridine linker **6** can be synthesized (**Scheme 3**) in 35% yield in one step starting from the comercially available terephthaldehyde and 2-acetylpyridine in the presence of KOH and NH_4OH in MeOH. The linker 7 can be obtained by the condensation reaction between the 4-thiomethylbenzaldehyde and 2-acetyl pyridine in the presence of the potassium tert-butoxide in THF, followed by its reaction with NH_4OAc to yield compound 7 in 75% yield. Deprotection of the methyl group was achieved by adding NaSEt to the refluxing solution of 7 to obtain compound **8** in 50% yield.

Currently, we are investigating the formation of these self-assembled molecular wires within the OWL-generated nanogaps. We are aiming two different routes for the assembly process in the OWLs which are pre-functionalized with the compound **8**. These are: (1) one-pot formation—addition of a metal salt and the bisterpyridine linker **6** to the solution at the same time and (2) step-wise formation—addition of a metal salt and the bisterpy linker sequentially. We have chosen Co(II) and Fe(II) as metal centers on

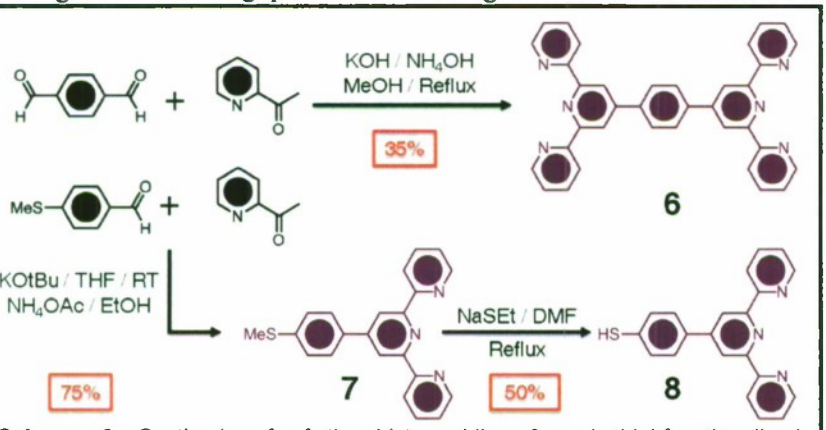

Scheme 3. Synthesis of of the bisterpyridine **6** and thiol-functionalized terpyridine **8**.

account of their both low-lying energy states and easy coordination reaction to the terpyridine ligand, i.e., at room temperature. In a typical one-pot formation experiment, devices incorporating OWL-generated nanogaps, which are functionalized with compound **8** by keeping them in a THF solution for 12 h, were immersed into a mixture (25 mM) of $Co(OAc)_2$ or $Fe(OAc)_2$ salts and the bisterpyridine linker **6** in MeOH. The mixture was refluxed at 60 °C for 3 h—in which color changes were observed consistent with the formation of molecular wires in solution—and subsequently rinsed with CH_2Cl_2, THF, and EtOH thoroughly. These devices are being tested and we have obtained *I–V* responses in our preliminary tests on some of the devices. We are currently working on the step-wise approach in order to further support our hypothesis that observed *I–V* response results from molecular wires that are only located inside the nanogaps. In this approach, nanowires functionalized with compound **8** will be immersed firstly into refluxing solutions of Co(II) or Fe(II) ions in MeOH, and then transferred into refluxing solution of bisterpyridine linker **6** in $CHCl_3$. These steps will be repeated until the formation of molecular wires inside the nanogaps is completed which is monitored by an *I–V* response. These experiments are under investigation.

Objective 5: Photoinduced Memory Effect in a Redox Controllable Bistable Mechanical Molecular Switch

We have demonstrated recently the performance of a molecular switch in the form of a bistable [2]rotaxane (Scheme 4), which (i) undergoes relative mechanical movements of its ring and dumbbell components under redox control and thus can be switched between two states thermodynamically, and wherein (ii) the energy barriers between these two states can be controlled kinetically by photochemical means, thus resulting in a bistable memory element.

The template-directed strategy, which was employed in the synthesis of *trans*-**1**•4PF_6, is outlined in Scheme 4. The TTF derivative **9** bearing an azide, and the azobenzene derivative *trans*-**10**, incorporating a DNP unit and a terminal alkyne were obtained in relatively high yields in three and one steps, respectively. The [2]rotaxane *trans*-**1**•4PF_6 was isolated in 35% yield, following the reaction of **9** with *trans*-**10** in Me_2CO using a copper(I)-catalyzed azide-alkyne cycloaddition (CuAAC) in the presence of **CBPQT**·4PF_6, while relying upon a threading-followed-by-stoppering

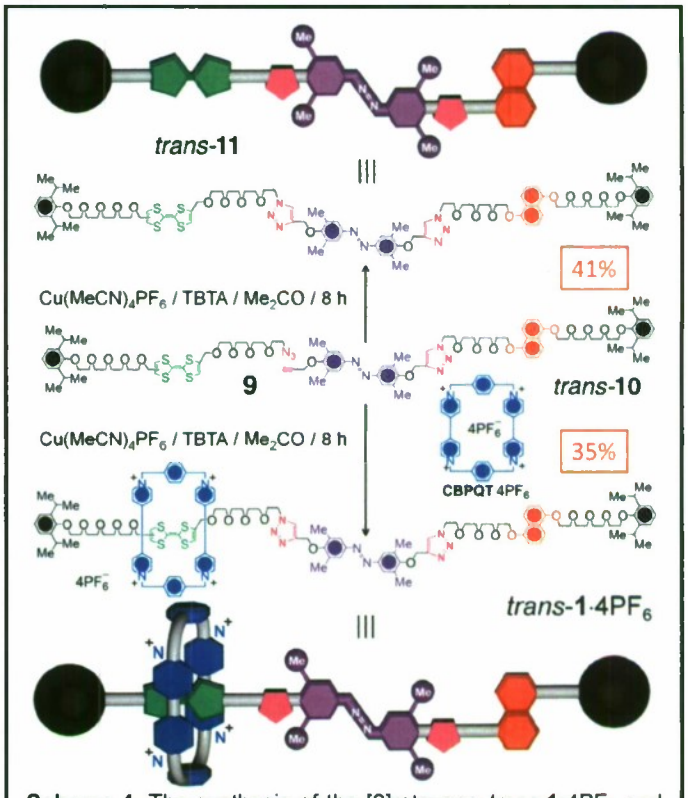

Scheme 4. The synthesis of the [2]rotaxane *trans*-**1**•4PF_6 and the corresponding dumbbell *trans*-**11**—along with their graphical representations.

approach to form the [2]rotaxane. The resulting [2]rotaxane was characterized by NMR spectroscopy and mass spectrometry. The ^{1}H NMR spectrum of *trans*-**1**•4PF$_6$ in CD_3CN reveals that the CBPQT^{4+} ring prefers to reside on the TTF unit as opposed to on the DNP one in an approximately 9:1 ratio. The simple dumbbell *trans*-**11** was obtained under similar experimental conditions in 41% yield.

The design of [2]rotaxane $\mathbf{1}^{4+}$ is based on a well-studied architecture in which the ring component is cyclobis(paraquat-*p*-phenylene) (CBPQT^{4+}) and the dumbbell component is comprised of (i) a tetrathiafulvalene (TTF) unit and a 1,5-dioxynaphthalene (DNP) unit as the primary and secondary π-electron-donating recognition sites, respectively, for the π-electron deficient CBPQT^{4+} ring, and (ii) a photoactive 3,5,3',5'-tetramethylazobenzene (TMeAB) unit, which can be switched between its cis and trans configurations reversibly and efficiently by photochemical stimuli, located in between the TTF and DNP units. Since the TTF unit is more π–electron–rich than the DNP one, the CBPQT4+ ring prefers to reside on the TTF unit rather than on the DNP unit in the ground state co-conformation (GSCC) of $\mathbf{1}^{4+}$. Upon chemical or electrochemical oxidation of the TTF unit to its radical cation (TTF$^{\bullet+}$) form, the CBPQT^{4+} ring shuttles to the DNP recognition site on account of the Coulombic repulsion between the ring and the oxidized TTF unit, namely the TTF$^{\bullet+}$ radical cation. Upon reduction of the TTF$^{\bullet+}$ unit to its neutral state, the CBPQT^{4+} ring resides on the DNP recognition site (metastable state co-conformation, MSCC) for some time before its relaxation to the GSCC is complete. The lifetime of the MSCC can be controlled (Figure 6) by the isomerization of TMeAB unit from its trans to cis configuration, a process which brings about a large geometrical change capable of affecting substantially the free energy barrier for the shuttling of the CBPQT^{4+} ring along the dumbbell component, given that a cis azobenzene unit poses a much larger steric hindrance to the shuttling of the ring than does a trans azobenzene unit. We have performed *in situ* oxidation-photoirradiation-reduction-thermal reset experiments in order to explore the possibility of trapping the shuttle in the MSCC by photochemically closing the azobenzene gate when the CBPQT^{4+} ring resides on the DNP secondary recognition site. Specifically, we anticipated that (i) chemical oxidation causes the shuttling of the CBPQT^{4+} ring from the TTF$^{\bullet+}$ to the DNP recognition site, (ii) light irradiation converts the TMeAB unit from a *trans* to a *cis* configuration (gate closed), (iii) successive chemical reduction regenerates the neutral TTF unit with the CBPQT^{4+} ring still residing on the DNP unit, and (iv) thermal *cis*→*trans* isomerization opens the gate and allows the repositioning

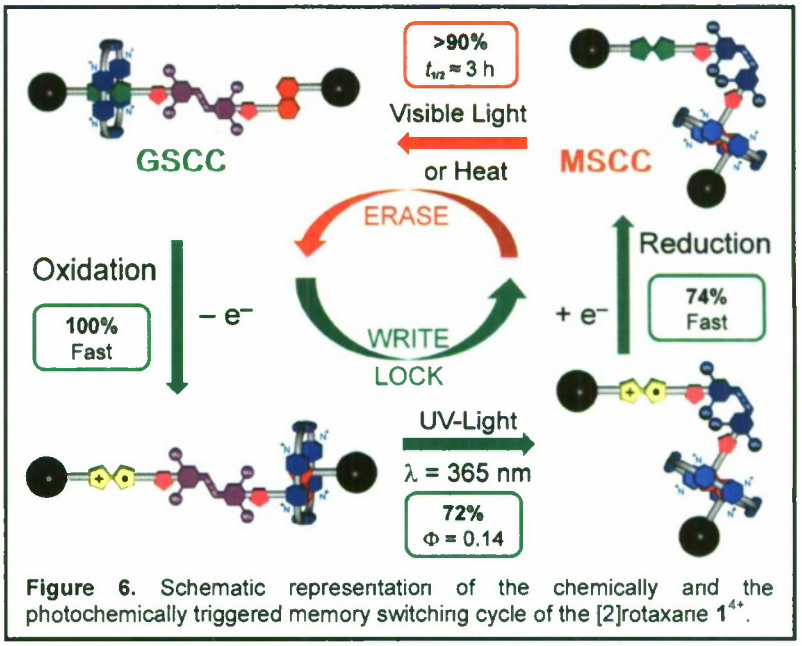

Figure 6. Schematic representation of the chemically and the photochemically triggered memory switching cycle of the [2]rotaxane $\mathbf{1}^{4+}$.

of the $CBPQT^{4+}$ ring onto the TTF primary recognition site, thereby affording (Figure 6) full reset of the system. With the promising solution-state results in hand, the work towards integration of a similar system into nanogaps is in progress in order to obtain a memory device.

Publications

(1) Avellini, T.; Hao, L.; Coskun, A.; Barin, G.; Trabolsi, A.; Basuray, A. N.; Dey, S. K.; Credi, A.; Silvi, S.; Stoddart, J. F.; Venturi, M. "Photoinduced Memory Effect in a Redox Controllable Bistable Molecular Switch," *Angew. Chem. Int. Ed.*, **2012**, *DOI: 10.1002/anie.201107618.*

Presentations

Chad Mirkin:

(1) Pacifichem, Honolulu, HI:
"Nanostructure Synthesis with Plasmonic Seeds", **"Coordination-Based Abiotic Molecular Machines"**, and **"Novel Forms of Biolabeling and Amplification Afforded by Structures Generated by On-Wire Lithograph,"** (2010).

(2) Bio-X STT-TAGGANTS Review, Dayton, OH:
"Biobarcodes and Nanoflares: New Nanotechnological Taggant Approaches," (2011)

(3) 10^{th} US-Korea Workshop on Nanostructured Materials, 8^{th} US-Korea Workshop on Nanoelectronics, and NBIT Program Review, Gyeongiu, Republic of Korea:
"Massively Parallel Nanostructure Assembly," (2011).

Fraser Stoddart:

(1) Samsung Technical Conference 2010, Hotel Shilla, Seoul, Republic of Korea:
"An Integrated Mechanostereochemical Systems Approach to Molecular Electronics" (2010)

(2) JSPS Second International Symposium on Molecular Nanotechnology, Nara, Japan:
"Fashioning Functional Materials with Integrated Mechanostereochemical Systems" (2010)

(3) Chemistry Colloquium Speaker, Pennsylvania State University, State College, PA:
"An Integrated Mechanostereochemical Approach to Molecular Electronics" (2011)

(4) CSACS Lecturer at INRS, Varennes, Canada:
"An Integrated Mechanostereochemical Approach to Molecular Electronics" (2011)